 CMC, vol.44, no.3, pp.141-166, 2014

Computing the Electric and Magnetic Green's Functions in General Electrically Gyrotropic Media

V. G. Yakhno[1], B. Çiçek[2]

Abstract: A method for an approximate computation of the electric and magnetic Green's functions for the time-harmonic Maxwell's equations in the general electrically gyrotropic materials is proposed. This method is based on the Fourier transform meta-approach: the equations for electric and magnetic fields are written in terms of images of the Fourier transform with respect to space variables and as a result of it the linear algebraic systems for finding Fourier images of the columns of the Green's functions are obtained. The explicit formulas for the solutions of the obtained systems have been found. Finally, elements of the Green's functions are determined by the inverse Fourier transform in the space of tempered distributions. The approximate computation of the inverse Fourier transform has been implemented by MATLAB tools. The computational experiments confirm the robustness of the method.

Keywords: Gyro-electric materials, Green's functions, analytical method, simulation.

1 Introduction

The Faraday effect, observed in 1945 in a piece of glass placed between the poles of a magnet, was the first of the magneto-optical effects to be discovered by Michael Faraday [Faraday (1933)]. The result of the existence of magnetic fields inside of magneto-optical materials opens gyrotropic materials. Gyrotropic materials have been an active research topic because, using these materials, new microwave devices such as circulators, isolators, resonators, and optical devices such as modulators, switches, phase shifters can be designed [Eroglu (2003); Eroglu (2006a); Eroglu (2006b)]. Moreover, the study of electromagnetic wave propagation in gyrotropic materials can be used in development of gyrotropic devices for ionospheric

[1] Electrical and Electronics Engineering Department, Dokuz Eylul University, Kaynaklar, Buca, Izmir, 35160, Turkey.

[2] Mathematics Department, The Graduate School of Natural and Applied Sciences, Dokuz Eylul University, Kaynaklar, Buca, Izmir, 35160, Turkey.

applications [Eroglu (2006b)]. The electromagnetic fields observed in magnetically biased plasma or ferrite can be modeled as electromagnetic waves in gyrotropic materials [Eroglu (2006b)]. Many problems of remote sensing, monolithic integrated circuits and optics, geophysical probing, microstrip circuits and antennas, submarine communication, opto-electronics etc. are connected with electromagnetic fields in gyro-electric materials [Eroglu (2010); Eroglu (2003); Eroglu (2006a); Eroglu (2006b); Prati (2003)].

If the electrical and/or magnetic properties of a medium depend upon the directions of field vectors, then the medium is called anisotropic medium and the relationships between fields have the following form

$$\mathbf{D} = \varepsilon_0 \bar{\bar{\varepsilon}} \mathbf{E},$$
$$\mathbf{B} = \mu_0 \bar{\bar{\mu}} \mathbf{H},$$

where $\bar{\bar{\varepsilon}}$ and $\bar{\bar{\mu}}$ are relative permittivity and permeability matrices, respectively. ε_0 and μ_0 are defined as the permittivity and permeability of free space [Eroglu (2010); Kong (1984)].

Anisotropic materials may be divided into two classes, depending on whether the natural modes of propagation are linearly polarized or circularly polarized waves [Eroglu (2010)]. In the first class, the permittivity and permeability components are symmetric; that is $\varepsilon_{ik} = \varepsilon_{ki}$ and $\mu_{ik} = \mu_{ki}$. For the second class, called gyrotropic media, the permittivity or permeability matrices are Hermitian, that is $\varepsilon_{ij} = \varepsilon_{ji}^*$ and $\mu_{ij} = \mu_{ji}^*$, where * is denoted as complex conjugate of the given element.

The gyrotropic medium becomes *electrically gyrotropic* or *gyro-electric* if the permittivity matrix $\bar{\bar{\varepsilon}}$ is Hermitian and the permeability matrix $\bar{\bar{\mu}} = \mu_0 I$. The gyrotropic medium becomes *magnetically gyrotropic* or *gyro-magnetic* if the permeability matrix $\bar{\bar{\mu}}$ is Hermitian and $\bar{\bar{\varepsilon}} = \varepsilon_0 I$ [Eroglu (2010); Kong (1984)].

In the present paper we consider the gyro-electric materials in the general form when the permittivity matrix can be written as the following matrix (see, for example, [Eroglu (2010)])

$$\bar{\bar{\varepsilon}} = \begin{pmatrix} \varepsilon_{11} & \varepsilon_{12} + ig_3 & \varepsilon_{13} - ig_2 \\ \varepsilon_{12} - ig_3 & \varepsilon_{22} & \varepsilon_{23} + ig_1 \\ \varepsilon_{13} + ig_2 & \varepsilon_{23} - ig_1 & \varepsilon_{33} \end{pmatrix}, \tag{1}$$

and $\bar{\bar{\mu}} = \mu_0 I$. The main objects of our paper are the electric and magnetic Green's functions for Maxwell's partial differential equations in the general gyro-electric media. Green's functions for equations of mathematical physics can be considered as a useful tool for different methods in the presentation of acoustic, electromagnetic, elastic and other fields, in particular, for the method of moments

and boundary element method [Tai (1994); Kong (1984); Lindell (1994); Chew (1990); Tewary (1995);Tewary (2004); Rashed (2004); Gu (2009); Chen (2009); Yang (2008); Young (2005); Yakhno (2011b); Yakhno (2011a); Yakhno (2012); Yakhno (2013)] . When the dyadic Green's functions can be constructed it leads to the significant simplification of modelling electromagnetic waves and allows engineers to overcome calculational difficulties [Tewary (2002)]. The existence proofs for fundamental solutions (infinite-body Green's functions) in the spaces of generalized functions (tempered distributions) for any linear differential equations with constant coefficients were given by [Malgrange (1956); Ehrenpreis (1960); Hormander (1963)]. The proofs were based on the Fourier transform meta-approach consisting of the application of the Fourier transform with respect to the space variables. As a result, the equations for the image of the fundamental solutions depending on the Fourier parameters were found. Finally, to get the fundamental solution it is necessary to apply the inverse Fourier transform to this image with respect to parameters of the Fourier transform. This inverse Fourier transform is defined in the space of tempered distribution only. Generally speaking, tempered distributions do not have values at fixed points and can not be presented in the graphic form (as graphs). Moreover, the inverse Fourier transform in the space of tempered distributions is presented in the form of the divergent integrals in the classical sense. Using the technique of generalized functions the inverse Fourier transform of the Fourier images has been calculated analytically in the space of the tempered distributions for some scalar partial differential equations with constant coefficients (see, for example, [Vladimirov (1971)]). As result the explicit formulae of the fundamental solutions for these partial differential equations have been obtained.

Let us mention some works related to the construction of the Green's functions for equations of electromagnetics. Ortner and Wagner [Ortner (2004)], Wagner [Wagner (2011)] have applied the Fourier meta-approach and found the explicit formulae of the Green's functions for the systems of elasticity and Maxwell's equations for some particular cases of anisotropy only by the Fourier transform meta-approach. These formulae can be used for the computer implementation. The approximate computation of the time-dependent three-dimensional Green's functions (fundamental solutions) in general anisotropic materials by the Fourier transform meta-approach was suggested in the papers [Yakhno (2008); Yakhno (2011b)]. Using the Lorentz reciprocity relation and the multiple scattering approach the dyadic Green's functions for gyro-electric media are found in [Barkleshli (1993)]. The dyadic Green's functions for an electrically gyrotropic medium with particular form of $\bar{\bar{\varepsilon}}$ have been derived by matrix method with dyadic decomposition in [Eroglu (2003); Eroglu (2006a); Eroglu (2006b)]. The time-harmonic Green's dyadics have been constructed in closed form for a particular case of homogeneous gyrotropic mate-

rials by Fourier transform approach in [Olyslager (1997)].

However, the numerical computation of the Green's functions (fundamental solutions) of Maxwell's equations in general gyro-electric materials is not known. Moreover the numerical methods for the space of tempered distributions are not developed till now.

In our paper we suggest a method of an approximate (regularized) computation of the infinite-body Green's functions for the time-harmonic Maxwell's equations in the general gyro-electric materials. This method is based on the Fourier transform meta-approach where the Fourier image of the Green's function is computed by some matrix transformations and symbolic computations in MATLAB. After that the inverse Fourier transform is computed in an regularized (approximate) form. The parameters of the regularization have been chosen by the comparison of the regularized Green's function with Green's function obtained by the explicit formula for the isotropic case. The approximate computation of the inverse Fourier transform has been implemented by MATLAB tools. The computational experiments are presented in the paper.

The paper is organized as follows. The equations for the time-harmonic electric and magnetic Green's functions are written in the beginning of Section 2. Methods of computing the electric and magnetic Green's functions are described in Section 2.1 and 2.2 respectively. Computational experiments are described in Section 3.

2 Electric and Magnetic Green's Functions in General Gyro-electric Media

The electric Green's function is a matrix function

$$\begin{pmatrix} E_1^1(x) & E_1^2(x) & E_1^3(x) \\ E_2^1(x) & E_2^2(x) & E_2^3(x) \\ E_3^1(x) & E_3^2(x) & E_3^3(x) \end{pmatrix}, \tag{2}$$

whose columns $\mathbf{E}^{\mathbf{k}} = (E_1^k, E_2^k, E_3^k)^T$ satisfy the equation

$$-\omega^2 \varepsilon_0 \mu_0 \bar{\bar{\varepsilon}} \mathbf{E}^{\mathbf{k}}(x,\omega) + \nabla \times \left(\nabla \times \mathbf{E}^{\mathbf{k}}(x,\omega)\right) = i\omega\mu_0 \mathbf{e}^{\mathbf{k}} \delta(x). \tag{3}$$

The magnetic Green's function is a matrix function

$$\begin{pmatrix} H_1^1(x) & H_1^2(x) & H_1^3(x) \\ H_2^1(x) & H_2^2(x) & H_2^3(x) \\ H_3^1(x) & H_3^2(x) & H_3^3(x) \end{pmatrix}, \tag{4}$$

whose columns $\mathbf{H}^{\mathbf{k}} = (H_1^k, H_2^k, H_3^k)^T$ satisfy the equation

$$-\omega^2 \varepsilon_0 \mu_0 \mathbf{H}^{\mathbf{k}}(x,\omega) + \nabla \times \left(\bar{\bar{\varepsilon}}^{-1} \nabla \times \mathbf{H}^{\mathbf{k}}(x,\omega)\right) = \nabla \times (\bar{\bar{\varepsilon}}^{-1} \mathbf{e}^{\mathbf{k}} \delta(x)). \tag{5}$$

Here $x=(x_1,x_2,x_3)\in\mathbb{R}^3$ is the $3D$ space variable; ω is a fixed parameter (frequency); $\varepsilon_0=8.854\times10^{-12}F/m$, $\mu_0=1.257\times10^{-6}N/A^2$ are positive constants (dielectric permittivity and magnetic permeability) of vacuum, respectively; $\mathbf{e}^1=(1,0,0)^T$, $\mathbf{e}^2=(0,1,0)^T$, $\mathbf{e}^3=(0,0,1)^T$ are basis vectors of $\mathbb{R}^3$; i is the imaginary unit $i^2=-1$; $\delta(x)=\delta(x_1)\delta(x_2)\delta(x_3)$, $\delta(x_j)$ is the Dirac delta function concentrated at $x_j=0$ for $j=1,2,3$.

2.1 Computing the Electric Green's function

Let $\mathscr{F}_x$ be the operator of the Fourier transform with respect to $x=(x_1,x_2,x_3)$, i.e.

$$\mathscr{F}_x[E(x)](\nu)=\int_{-\infty}^{\infty}\int_{-\infty}^{\infty}\int_{-\infty}^{\infty}E(x)e^{i\nu\cdot x}dx_1dx_2dx_3\,,$$

for the scalar integrable function $E(x)$, where $\nu=(\nu_1,\nu_2,\nu_3)$ is a $3D$ parameter of the Fourier transform; $\nu\cdot x=\nu_1x_1+\nu_2x_2+\nu_3x_3$. The operator of the Fourier transform is defined in [Vladimirov (1979)] for any generalized function (tempered distribution).

Let $\widetilde{\mathbf{E}}^{\mathbf{k}}(\nu)=(\widetilde{E}_1^k,\widetilde{E}_2^k,\widetilde{E}_3^k)$, where $\widetilde{E}_j^k=\mathscr{F}_x[E_j^k(x)](\nu)$, $j,k=1,2,3$. Applying the operator of the Fourier transform $\mathscr{F}_x$ to (3) and using equality (see, [Yakhno (2008)], page 415)

$$\mathscr{F}_x\big[\nabla\times(\nabla\times\mathbf{E}^{\mathbf{k}}(x))\big]=A(\nu)\widetilde{\mathbf{E}}^{\mathbf{k}}(\nu)\,,$$

we find

$$-\omega^2\varepsilon_0\mu_0\bar{\bar{\varepsilon}}\,\widetilde{\mathbf{E}}^{\mathbf{k}}(\nu)+A(\nu)\widetilde{\mathbf{E}}^{\mathbf{k}}(\nu)=i\omega\mu_0\mathbf{e}^{\mathbf{k}}\,, \tag{6}$$

where

$$A(\nu)=\begin{pmatrix}\nu_2^2+\nu_3^2 & -\nu_1\nu_2 & -\nu_1\nu_3\\ -\nu_1\nu_2 & \nu_1^2+\nu_3^2 & -\nu_2\nu_3\\ -\nu_1\nu_3 & -\nu_2\nu_3 & \nu_1^2+\nu_2^2\end{pmatrix}. \tag{7}$$

Let ε be a symmetric real 3×3 matrix and g be an antisymmetric real 3×3 matrix defined by

$$\varepsilon=\begin{pmatrix}\varepsilon_{11} & \varepsilon_{12} & \varepsilon_{13}\\ \varepsilon_{12} & \varepsilon_{22} & \varepsilon_{23}\\ \varepsilon_{13} & \varepsilon_{23} & \varepsilon_{33}\end{pmatrix},\quad g=\begin{pmatrix}0 & g_3 & -g_2\\ -g_3 & 0 & g_1\\ g_2 & -g_1 & 0\end{pmatrix}. \tag{8}$$

The matrix $\bar{\bar{\varepsilon}}$ defined by (1) can be written as $\bar{\bar{\varepsilon}}=\varepsilon+ig$. Further, let B and $C(\nu)$ be symmetric 6×6 matrices defined by

$$B=\begin{pmatrix}\varepsilon & -g\\ g & \varepsilon\end{pmatrix},\quad C(\nu)=\begin{pmatrix}A(\nu) & 0\\ 0 & A(\nu)\end{pmatrix}. \tag{9}$$

In the paper we suppose that B is positive definite.

Remark 2.1 *Positive definiteness of B is natural for a wide class of gyrotropic materials because the matrix ε is always positive definite and the elements of matrix g essentially smaller then elements of ε (see, for example, [Freiser (1968)]; [Pershan (1967)]).*

Moreover under assumption of positive definiteness of B the matrix $\bar{\bar{\varepsilon}}$ is invertible, i.e. the inverse matrix $\bar{\bar{\varepsilon}}^{-1}$ exists.

Let us denote V_j^k as the real part of j component of $\widetilde{\mathbf{E}}^{\mathbf{k}}(\nu)$ and V_{j+3}^k as the imaginary part of j component of $\widetilde{\mathbf{E}}^{\mathbf{k}}(\nu)$, i.e. $V_j^k = Re(\widetilde{E}_j^k(\nu))$ and $V_{j+3}^k = Im(\widetilde{E}_j^k(\nu))$, $j = 1,2,3$. Then equality (6) can be written as a vector equation

$$-\omega^2\varepsilon_0\mu_0 B\mathbf{V}^{\mathbf{k}}(\nu) + C(\nu)\mathbf{V}^{\mathbf{k}}(\nu) = \mathbf{F}^{\mathbf{k}}, \tag{10}$$

where $\mathbf{F^1} = \omega\mu_0(0,0,0,1,0,0)^T$, $\mathbf{F^2} = \omega\mu_0(0,0,0,0,1,0)^T$, $\mathbf{F^3} = \omega\mu_0(0,0,0,0,0,1)^T$. Applying technique and computational tools of [Yakhno (2011b)], it is possible to compute a non-singular matrix $T(\nu)$ and diagonal matrix $D(\nu) = diag(d_1(\nu), d_2(\nu), \ldots, d_6(\nu))$, such that

$$T^T(\nu)C(\nu)T(\nu) = D(\nu),$$
$$T^T(\nu)BT(\nu) = I.$$

(MATLAB code of this computation is given in Appendix A:).

Below the equation (10) is written in terms of a new unknown vector function $\mathbf{Y}^{\mathbf{k}}$ which is defined by

$$\mathbf{V}^{\mathbf{k}}(\nu) = T(\nu)\mathbf{Y}^{\mathbf{k}}(\nu). \tag{11}$$

Substituting (11) into (10) we find

$$-\omega^2\varepsilon_0\mu_0 BT(\nu)\mathbf{Y}^{\mathbf{k}}(\nu) + C(\nu)T(\nu)\mathbf{Y}^{\mathbf{k}}(\nu) = \mathbf{F}^{\mathbf{k}}. \tag{12}$$

Multiplying the equation (12) by $T^T(\nu)$, we find

$$-\omega^2\varepsilon_0\mu_0 I\mathbf{Y}^{\mathbf{k}}(\nu) + D(\nu)\mathbf{Y}^{\mathbf{k}}(\nu) = T^T(\nu)\mathbf{F}^{\mathbf{k}},$$

or in a component form

$$-\omega^2\varepsilon_0\mu_0 Y_l^k(\nu) + d_l(\nu)Y_l^k(\nu) = (T^T(\nu)\mathbf{F}^{\mathbf{k}})_l, \;\; l = 1,2,...,6. \tag{13}$$

For $\left(\frac{w}{c}\right)^2 - d_l(\nu) \neq 0$, the solution of (13) can be written as

$$Y_l^k(\nu) = \frac{(T^T \mathbf{F}^{\mathbf{k}})_l}{-(\omega/c)^2 + d_l(\nu)}, \tag{14}$$

where $l = 1,2,...,6$, $c = 1/\sqrt{\varepsilon_0 \mu_0}$. As a result, the solution of (10) is determined by

$$\mathbf{V}^{\mathbf{k}}(\nu) = T(\nu)\mathbf{Y}^{\mathbf{k}},$$

and the solution $\widetilde{\mathbf{E}}^{\mathbf{k}}(\nu,\omega)$ is found by

$$\widetilde{E}_j^k = V_j^k(\nu) + iV_{j+3}^k(\nu), j = 1,2,3; k = 1,2,3. \tag{15}$$

Finally, applying the inverse Fourier transform to (15), we find the k-column of the electric Green's function as a tempered distribution, i.e.

$$\mathbf{E}^{\mathbf{k}}(x) = \mathscr{F}_\nu^{-1}[\widetilde{\mathbf{E}}^{\mathbf{k}}(\nu)](x), \tag{16}$$

where $\mathscr{F}_\nu^{-1}$ is the operator of the inverse Fourier transform in the space of distribution $S'(\mathbb{R}^3)$ [Vladimirov (1979)].

Usually the classical functions are defined by a point-wise manner and we can draw their graphs. Unfortunately, this point-wise definition and its graphical presentation is not adequate to singular tempered distributions [Vladimirov (1979)]. They are very often replaced by regularized functions which are classical and have graphic presentations. This regularization has a parameter of the regularization and the singular generalized function is a limit in sense of the generalized functions space, when the parameter of the regularization tends to $+\infty$. The right hand side of (16) can be regularized by

$$\frac{1}{(2\pi)^3} \int_{-A}^{A} \int_{-A}^{A} \int_{-A}^{A} \widetilde{\mathbf{E}}^{\mathbf{k}}(\nu)\, e^{-i\nu\cdot x} d\nu_1 d\nu_2 d\nu_3, \tag{17}$$

where A is the parameter of regularization.

We take $A = N\Delta$ and approximate the integral (17) by the integral sum

$$\frac{1}{(2\pi)^3} \sum_{n=-N}^{N} \sum_{m=-N}^{N} \sum_{l=-N}^{N} \widetilde{\mathbf{E}}^{\mathbf{k}}(n\Delta, m\Delta, l\Delta)\, e^{-i\Delta(nx_1+mx_2+lx_3)} (\Delta\nu)^3, \tag{18}$$

for the numerical computation. The parameters N and Δ are determined by the procedure described in Section 3.2.

2.2 Computing the magnetic Green's function

Applying the Fourier transform with respect to x to the equation (5) and using equalities

$$\mathscr{F}_x\big[\nabla\times(\bar{\bar{\varepsilon}}^{-1}\nabla\times\mathbf{H}^{\mathbf{k}}(x))\big]=R(\nu)\bar{\bar{\varepsilon}}^{-1}R(\nu)\widetilde{\mathbf{H}}^{\mathbf{k}}(\nu),$$
$$\mathscr{F}_x\big[\nabla\times(\bar{\bar{\varepsilon}}^{-1}\mathbf{e}^{\mathbf{k}})\big]=R(\nu)\bar{\bar{\varepsilon}}^{-1}\mathbf{e}^{\mathbf{k}},$$

we find

$$-\omega^2\varepsilon_0\mu_0\widetilde{\mathbf{H}}^{\mathbf{k}}(\nu)+R(\nu)\bar{\bar{\varepsilon}}^{-1}R(\nu)\widetilde{\mathbf{H}}^{\mathbf{k}}(\nu)=R(\nu)\bar{\bar{\varepsilon}}^{-1}\mathbf{e}^{\mathbf{k}}, \tag{19}$$

where $\widetilde{\mathbf{H}}^{\mathbf{k}}(\nu)=(\widetilde{H}_1^k,\widetilde{H}_2^k,\widetilde{H}_3^k)$, $\widetilde{H}_n^k(\nu)=\mathscr{F}_x[H_n^k(x)](\nu)$, $n=1,2,3$; and

$$R(\nu)=\begin{pmatrix}0&-\nu_3&\nu_2\\ \nu_3&0&-\nu_1\\ -\nu_2&\nu_1&0\end{pmatrix}.$$

Let $X_n^k(\nu)$, $G_n^k(\nu)$, $S_r(\nu)$ be the real parts of $\widetilde{H}_n^k(\nu)$, $(R(\nu)\bar{\bar{\varepsilon}}^{-1}\mathbf{e}^{\mathbf{k}})$, $(R(\nu)\bar{\bar{\varepsilon}}^{-1}R(\nu))$ and $X_{n+3}^k(\nu)$, $G_{n+3}^k(\nu)$, $S_i(\nu)$ be the imaginary parts of $\widetilde{H}_n^k(\nu)$, $(R(\nu)\bar{\bar{\varepsilon}}^{-1}\mathbf{e}^{\mathbf{k}})$, $(R(\nu)\bar{\bar{\varepsilon}}^{-1}R(\nu))$, respectively.
Denoting $\mathbf{X}^{\mathbf{k}}(\nu)$=$(X_1^k(\nu),X_2^k(\nu),\ldots,X_6^k(\nu))$ and $\mathbf{G}^{\mathbf{k}}(\nu)$=$(G_1^k(\nu),G_2^k(\nu),\ldots,G_6^k(\nu))$ the equation (19) can be written in the form

$$-\omega^2\varepsilon_0\mu_0\mathbf{X}^{\mathbf{k}}(\nu)+P(\nu)\mathbf{X}^{\mathbf{k}}(\nu)=\mathbf{G}^{\mathbf{k}}(\nu), \tag{20}$$

where $P(\nu)$ is a 6×6 symmetric matrix defined by

$$P(\nu)=\begin{pmatrix}S_r(\nu)&-S_i(\nu)\\ S_i(\nu)&S_r(\nu)\end{pmatrix}. \tag{21}$$

We note that $(R(\nu)\bar{\bar{\varepsilon}}^{-1}R(\nu))=S_r(\nu)+iS_i(\nu)$, where

$$S_i(\nu)=\frac{1}{\xi_4}\begin{pmatrix}0&-a_{12}&a_{13}\\ a_{12}&0&-a_{23}\\ -a_{13}&a_{23}&0\end{pmatrix},\quad S_r(\nu)=\frac{1}{\xi_4}\begin{pmatrix}b_{11}&b_{12}&b_{13}\\ b_{12}&b_{22}&b_{23}\\ b_{13}&b_{23}&b_{33}\end{pmatrix},$$

$$a_{12}=\nu_2\nu_3\xi_1+\nu_3^2\xi_2+\nu_1\nu_3\xi_3,\ a_{13}=\nu_2^2\xi_1+\nu_2\nu_3\xi_2+\nu_1\nu_2\xi_3,$$
$$a_{23}=\nu_1\nu_3\xi_2+\nu_1^2\xi_3+\nu_1\nu_2\xi_1,$$
$$b_{11}=-\nu_2^2\xi_5+2\nu_2\nu_3\xi_6-\nu_3^2\xi_7,\ b_{12}=\nu_1\nu_2\xi_5-\nu_1\nu_3\xi_6-\nu_2\nu_3\xi_8+\nu_3^2\xi_9,$$
$$b_{13}=\nu_1\nu_3\xi_7-\nu_1\nu_2\xi_6-\nu_2^2\xi_8-\nu_2\nu_3\xi_9,\ b_{22}=-\nu_1^2\xi_5+2\nu_1\nu_3\xi_8-\nu_3^2\xi_{10},$$
$$b_{23}=\nu_2\nu_3\xi_{10}-\nu_1\nu_2\xi_8-\nu_1^2\xi_6+\nu_1\nu_3\xi_9,\ b_{33}=-\nu_1^2\xi_7+2\nu_1\nu_2\xi_8-\nu_2^2\xi_{10},$$

$$\xi_1 = \varepsilon_{12}g_1 + \varepsilon_{22}g_2 + \varepsilon_{23}g_3\,,\ \xi_2 = \varepsilon_{13}g_1 + \varepsilon_{23}g_2 + \varepsilon_{33}g_3\,,$$
$$\xi_3 = \varepsilon_{11}g_1 + \varepsilon_{12}g_2 + \varepsilon_{13}g_3\,,$$
$$\xi_4 = \varepsilon_{33}\varepsilon_{12}^2 - 2\varepsilon_{12}\varepsilon_{13}\varepsilon_{23} + 2\varepsilon_{12}g_1g_2 + \varepsilon_{22}\varepsilon_{13}^2 + 2\varepsilon_{13}g_1g_3 + \varepsilon_{11}\varepsilon_{23}^2 + 2\varepsilon_{23}g_2g_3$$
$$+ \varepsilon_{11}g_1^2 + \varepsilon_{22}g_2^2 + \varepsilon_{33}g_3^2 - \varepsilon_{11}\varepsilon_{22}\varepsilon_{33}\,,$$
$$\xi_5 = \varepsilon_{12}^2 + g_3^2 - \varepsilon_{11}\varepsilon_{22}\,,\ \xi_6 = g_2g_3 - \varepsilon_{12}\varepsilon_{13} + \varepsilon_{11}\varepsilon_{23}\,,\ \xi_7 = \varepsilon_{13}^2 + g_3^2 - \varepsilon_{11}\varepsilon_{33}\,,$$
$$\xi_8 = g_1g_3 - \varepsilon_{12}\varepsilon_{23} + \varepsilon_{13}\varepsilon_{22}\,,\ \xi_9 = g_1g_2 - \varepsilon_{13}\varepsilon_{23} + \varepsilon_{12}\varepsilon_{33}\,,$$
$$\xi_{10} = \varepsilon_{23}^2 + g_1^2 - \varepsilon_{22}\varepsilon_{33}\,. \tag{22}$$

Using the symbolic matrix transformation in MATLAB and the technique from [Yakhno (2011b)] we can compute an invertible matrix $Q(\nu)$ and $M(\nu)$ such that

$$Q^{-1}(\nu)Q(\nu) = I\,,$$
$$Q^{-1}(\nu)P(\nu)Q(\nu) = M(\nu)\,,$$

where $M(\nu) = diag(m_n(\nu)\,, n = 1,2,3,4,5,6)$. (MATLAB code of computation of $Q(\nu)$ and $M(\nu)$ is given in Appendix B:)
Let $\mathbf{Z^k}(\nu) = Q^{-1}(\nu)\mathbf{X^k}(\nu)$, then

$$\mathbf{X^k}(\nu) = Q(\nu)\mathbf{Z^k}(\nu)\,. \tag{23}$$

Using (23) the equation (20) can be written in the form

$$-\omega^2\varepsilon_0\mu_0 Q(\nu)\mathbf{Z^k}(\nu) + P(\nu)Q(\nu)\mathbf{Z^k}(\nu) = \mathbf{G^k}\,. \tag{24}$$

Multiplying the equation (24) by $Q^{-1}(\nu)$, we find

$$-\omega^2\varepsilon_0\mu_0\mathbf{Z^k}(\nu) + M(\nu)\mathbf{Z^k} = Q^{-1}(\nu)\mathbf{G^k}\,. \tag{25}$$

For $(\omega/c)^2 - m_n(\nu) \neq 0$ the solution of (25) can be written in a component form as follows

$$Z_n^k(\nu) = \frac{(Q^{-1}(\nu)\mathbf{G^k})_n}{-(\omega/c)^2 + m_n(\nu)}\,, \tag{26}$$

where $n = 1,2,...,6$. As a result the solution of (20) is determined by

$$\mathbf{X^k}(\nu) = Q(\nu)\mathbf{Z^k}\,,$$

and the solution of (19) is found by

$$\widetilde{H}_n^k = X_n^k(\nu) + iX_{n+3}^k(\nu)\,, j = 1,2,3\,; n = 1,2,3\,. \tag{27}$$

Applying the inverse Fourier transform to (27), we find the $k-$column of the magnetic Green's function as a tempered distribution, i.e.

$$\mathbf{H}^{\mathbf{k}}(x) = \mathscr{F}_{\nu}^{-1}[\widetilde{\mathbf{H}}^{\mathbf{k}}(\nu)](x)\,. \tag{28}$$

The right hand side of (28) can be regularized by

$$\frac{1}{(2\pi)^3}\int_{-A}^{A}\int_{-A}^{A}\int_{-A}^{A}\widetilde{\mathbf{H}}^{\mathbf{k}}(\nu)\,e^{-i\nu\cdot x}d\nu_1 d\nu_2 d\nu_3\,, \tag{29}$$

where A is the parameter of regularization.
We take $A = N\Delta$ and approximate the integral (29) by the integral sum

$$\frac{1}{(2\pi)^3}\sum_{n=-N}^{N}\sum_{m=-N}^{N}\sum_{l=-N}^{N}\widetilde{\mathbf{H}}^{\mathbf{k}}(\Delta n,\Delta m,\Delta l)\,e^{-i\Delta(nx_1+mx_2+lx_3)}(\Delta\nu)^3\,. \tag{30}$$

for the numerical computation. The parameters N and Δ are determined by the procedure described in Section 3.2.

3 Computational Examples

3.1 Computational accuracy of the Fourier transform of the electric Green's function

The Fourier transform of the electric and magnetic Green's functions can be found by exact formulas for the case of isotropic homogeneous materials. We use these formulas to compute the exact values of the Fourier transform of Green's functions and then to compare them with values computed by our method.
The components of $\widetilde{\mathbf{E}}^{\mathbf{k}}(\nu)=(\widetilde{\mathbf{E}}^{\mathbf{k}}_{\mathbf{1}}(\nu),\widetilde{\mathbf{E}}^{\mathbf{k}}_{\mathbf{2}}(\nu),\widetilde{\mathbf{E}}^{\mathbf{k}}_{\mathbf{3}}(\nu))$, $\widetilde{\mathbf{H}}^{\mathbf{k}}(\nu)=(\widetilde{\mathbf{H}}^{\mathbf{k}}_{\mathbf{1}}(\nu),\widetilde{\mathbf{H}}^{\mathbf{k}}_{\mathbf{2}}(\nu),\widetilde{\mathbf{H}}^{\mathbf{k}}_{\mathbf{3}}(\nu))$ satisfying equations (6) and (19) respectively for $k=1$ in the case of the isotropic homogeneous medium with permittivity ε_0 and permeability μ_0 are given by formulas

$$\widetilde{E}^1_1(\nu) = \frac{\frac{1}{i\omega\varepsilon_0}(-\nu_1^2)-i\omega\mu_0}{(\frac{\omega}{c})^2-|\nu|^2}\,,\ \widetilde{E}^1_2(\nu) = \frac{-\frac{1}{i\omega\varepsilon_0}\nu_1\nu_2}{(\frac{\omega}{c})^2-|\nu|^2}\,,\ \widetilde{E}^1_3(\nu) = \frac{-\frac{1}{i\omega\varepsilon_0}\nu_1\nu_3}{(\frac{\omega}{c})^2-|\nu|^2}\,, \tag{31}$$

$$\widetilde{H}^1_1(\nu) = 0\,,\ \widetilde{H}^1_2(\nu) = \frac{\nu_3}{(\frac{\omega}{c})^2-|\nu|^2}\,,\ \widetilde{H}^1_3(\nu) = \frac{-\nu_2}{(\frac{\omega}{c})^2-|\nu|^2}\,. \tag{32}$$

The functions $\widetilde{E}^1_j(\nu)$, $\widetilde{H}^1_j(\nu)$ defined by the explicit formulas (31), (32) will be denoted as $\widetilde{E}^e_j(\nu)$, $\widetilde{H}^e_j(\nu)$. The functions $\widetilde{E}^1_j(\nu)$, $\widetilde{H}^1_j(\nu)$ computed by our method for

the isotropic medium will be denoted as $\widetilde{E}_j^m(\nu)$, $\widetilde{H}_j^m(\nu)$. The results of computations of their values for $\omega = 1/\sqrt{\mu_0\varepsilon_0}$ and $\nu_1 = r\cos\phi\sin\theta$, $\nu_2 = r\sin\phi\sin\theta$, $\nu_3 = r\cos\theta$ for fixed $\theta = \pi/4$, $\phi = \pi/4$ and for fixed parameter r are presented in Table 1 and Table 2.

These computational experiments have shown that values of $\widetilde{E}_j^1$, $\widetilde{H}_j^1$ found by our method and by explicit formulas are almost the same (the accuracy is around 10^{-6}).

3.2 *Determining parameters for the approximate computation of the Fourier transform in the space of generalized functions*

The fundamental solution of the Helmholtz equation as well as the image of the Fourier transform with respect to a space variable are given by explicit formulas. We apply these explicit formulas to determine the parameters which we use for the numerical computation of the inverse Fourier transform for finding the electric and magnetic Green's functions in gyro-electric media.

Let us consider the fundamental solution

$$U(x) = -\frac{e^{i\omega|x|/c}}{4\pi|x|}, \quad x = (x_1, x_2, x_3), \tag{33}$$

of the Helmholtz equation

$$\omega^2 U(x) + c^2 \Delta U = \delta(x). \tag{34}$$

Applying the Fourier transform (the Fourier transform of generalized functions [Vladimirov (1979)]) to equation (34), we find

$$\omega^2 \widetilde{U}(\nu) - c^2|\nu|^2 \widetilde{U}(\nu) = 1,$$

where $\nu = (\nu_1, \nu_2, \nu_3) \in \mathbb{R}^3$ is the parameter of the Fourier transform, $|\nu|^2 = \nu_1^2 + \nu_2^2 + \nu_3^2$.

For $c^2|\nu|^2 - \omega^2 \neq 0$ we have

$$\tilde{U}(\nu) = \frac{1}{\omega^2 - c^2|\nu|^2}. \tag{35}$$

The fundamental solution $U(x)$, defined by (33), can be found by application of the inverse Fourier transform (as the inverse Fourier transform of generalized functions [Vladimirov (1979)]) to $\tilde{U}(\nu)$ determined by (35).

For the approximate computation $U_{N,\Delta}(x)$ of the function $U(x)$ we apply the approximation of the inverse Fourier transform by

$$\frac{1}{(2\pi)^3} \sum_{n=-N}^{N} \sum_{m=-N}^{N} \sum_{l=-N}^{N} \frac{1}{\omega^2 - c^2\Delta^2(n^2+m^2+l^2)} e^{-i\Delta(nx_1+mx_2+lx_3)} (\Delta\nu)^3. \tag{36}$$

Table 1: Analysis for **imaginary part** of $\widetilde{E}$ for isotropic case (r is a fixed parameter).

r	$\widetilde{E}_1^m$	$\lvert\widetilde{E}_1^m-\widetilde{E}_1^e\rvert$	$\widetilde{E}_2^m$	$\lvert\widetilde{E}_2^m-\widetilde{E}_2^e\rvert$	$\widetilde{E}_3^m$	$\lvert\widetilde{E}_3^m-\widetilde{E}_3^e\rvert$
10^{-4}	$-0.37678x10^{3}$	0	$0.94197x10^{-6}$	$0.18990x10^{-13}$	$0.13321x10^{-5}$	$0.44490x10^{-13}$
10^{-3}	$-0.37678x10^{3}$	0	$0.94197x10^{-6}$	$0.15462x10^{-14}$	$0.13321x10^{-3}$	$0.21486x10^{-13}$
10^{-2}	$-0.37681x10^{3}$	$0.56843x10^{-13}$	$0.94206x10^{-2}$	$0.53030x10^{-14}$	$0.13322x10^{-1}$	$0.44632x10^{-13}$
10^{-1}	$-0.37964x10^{3}$	$0.56843x10^{-13}$	$0.56843x10^{-1}$	$0.81046x10^{-14}$	$0.13456x10^{-1}$	$0.11324x10^{-13}$
0	$-0.37678x10^{3}$	0	0	0	0	0
10^{1}	$-0.91342x10^{2}$	$0.13073x10^{-11}$	$-0.95148x10^{2}$	$0.12931x10^{-11}$	$-1.34560x10^{2}$	$0.18474x10^{-11}$
10^{2}	$-0.94168x10^{2}$	$0.17135x10^{-9}$	$-0.94206x10^{2}$	$0.17136x10^{-9}$	$-1.33228x10^{2}$	$0.24232x10^{-9}$
10^{3}	$-0.94196x10^{2}$	$0.10965x10^{-7}$	$-0.94197x10^{2}$	$0.10965x10^{-7}$	$-1.33215x10^{2}$	$0.15508x10^{-7}$
10^{4}	$-0.94197x10^{2}$	$0.70182x10^{-6}$	$-0.94197x10^{2}$	$0.70182x10^{-6}$	$-1.33214x10^{2}$	$0.99252x10^{-6}$

Table 2: Analysis for **real** part of $\widetilde{H}$ for isotropic case (r is a fixed parameter).

r	$\widetilde{H}_1^m$	$\lvert\widetilde{H}_1^m-\widetilde{H}_1^e\rvert$	$\widetilde{H}_2^m$	$\lvert\widetilde{H}_2^m-\widetilde{H}_2^e\rvert$	$\widetilde{H}_3^m$	$\lvert\widetilde{H}_3^m-\widetilde{H}_3^e\rvert$
10^{-4}	$-0.13552x10^{-21}$	$0.13552x10^{-21}$	$-0.70710x10^{-6}$	$0.14142x10^{-14}$	$0.49999x10^{-6}$	$0.99999x10^{-14}$
10^{-3}	$-0.81315x10^{-21}$	$0.81315x10^{-21}$	$-0.70710x10^{-5}$	$0.14142x10^{-10}$	$0.49999x10^{-5}$	$0.99999x10^{-11}$
10^{-2}	$0.86736x10^{-20}$	$0.86736x10^{-20}$	$-0.70703x10^{-5}$	$0.14142x10^{-7}$	$0.49999x10^{-5}$	$0.10000x10^{-7}$
10^{-1}	$0.17347x10^{-18}$	$0.17347x10^{-18}$	$0.70010x10^{-4}$	$0.14143x10^{-5}$	$0.49505x10^{-4}$	$0.10001x10^{-5}$
0	0	0	0	0	0	0
10^{1}	$-0.15196x10^{-16}$	$0.15196x10^{-16}$	$0.70010x10^{-4}$	$0.14143x10^{-5}$	$0.49505x10^{-4}$	$0.10001x10^{-5}$
10^{2}	$-0.71032x10^{-16}$	$0.71032x10^{-16}$	$-0.70703x10^{-5}$	$0.14142x10^{-7}$	$0.49995x10^{-5}$	$0.10000x10^{-7}$
10^{3}	$-0.28421x10^{-15}$	$0.28421x10^{-15}$	$-0.70710x10^{-6}$	$0.14141x10^{-10}$	$0.49999x10^{-5}$	$0.10000x10^{-10}$
10^{4}	$0.45474x10^{-14}$	$0.45474x10^{-14}$	$-0.707106x10^{-6}$	$0.186896x10^{-13}$	$0.50000x10^{-6}$	$0.35689x10^{-14}$

The parameters N and Δ have been chosen using the empirical observation and natural logic. Namely, using the formula (36) we compute values $U_{N,\Delta}(x)$ for $\Delta = 0.1, 0.5, 0.8, 1.0$, $N = 20, 30, 40, 50, 60, 80$ and so on numerically in MATLAB. We compare the computed values of $U_{N,\Delta}(x)$ with values of the function $U(x)$, defined by (33). We have observed that the difference between the values of $U_{N,\Delta}(x)$ and $U(x)$ corresponding to $\Delta = 1$ and $N = 30, 40, 50, 60, 80, 100$ becomes small and increment of the approximation for the parameter N is not essential, according to the case $\Delta = 1$, $N = 30$. For this reason we choose $\Delta = 1$, $N = 30$ as the suitable parameters for the calculation of the inverse Fourier transform by (36).

We have presented $1D$ graphs of the functions $U(x)$ and $U_{N,\Delta}(x)$ for the different values of N and Δ in Fig. 1 and Fig. 2.

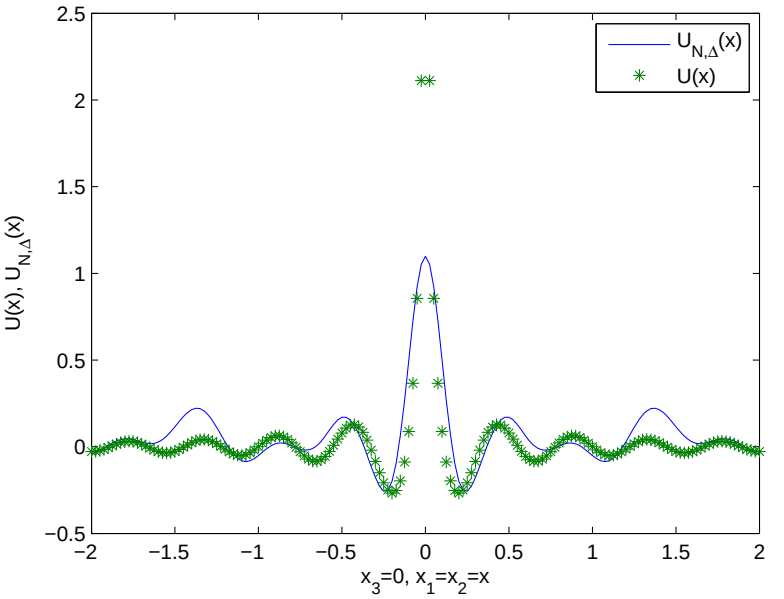

Figure 1: $1D$ plot of $U(x)$ and $U_{N,\Delta}(x)$ for $N = 30$, $\Delta = 0.5$

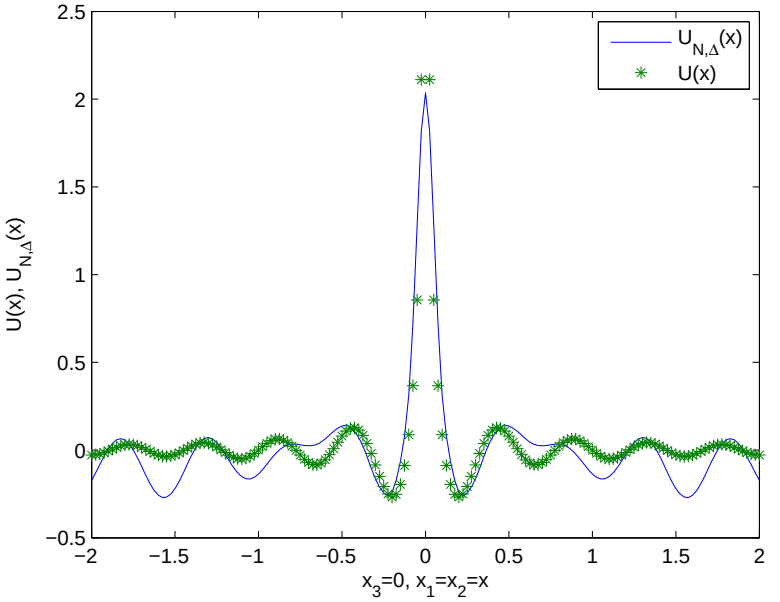

Figure 2: $1D$ plot of $U(x)$ and $U_{N,\Delta}(x)$ for $N = 30$, $\Delta = 1.0$

3.3 The approximate computation of the electric and magnetic Green's functions in general gyro-electric media

In this section we consider the computation of electric and magnetic Green's functions for general gyro-electric media characterizing by

$$\bar{\bar{\varepsilon}} = \begin{pmatrix} 30.7929 & -12.7337 + i0.5\,\kappa & -14.3432 - i0.4\,\kappa \\ -12.7337 - i0.5\,\kappa & 5.51479 & 5.86982 + i0.2\,\kappa \\ -14.3432 + i0.4\,\kappa & 5.86982 - i0.2\,\kappa & 6.74556 \end{pmatrix} \tag{37}$$

where $\kappa = 10^{-1}$ and 10^{-2}.

Applying the method of Section 2.1 we have computed $T(\nu)$, $T^T(\nu)$, $D(\nu)$ and then using the formula (18) we have derived solutions $\mathbf{E^1}(x)$, $\mathbf{E^2}(x)$, $\mathbf{E^3}(x)$ of (6) numerically and applying the method of Section 2.2 we have computed $Q(\nu)$, $Q^{-1}(\nu)$, $M(\nu)$ and then using the formula (30) we have derived solutions $\mathbf{H^1}(x)$, $\mathbf{H^2}(x)$, $\mathbf{H^3}(x)$ of (19) numerically.

Results of the computation of real and imaginary parts of $E_1^1(x)$, $E_2^1(x)$ and $H_1^1(x)$, $H_2^1(x)$ for $\kappa = 10^{-1}, 10^{-2}$ are presented in Fig. 3, Figs. 5-6 and Fig. 4, Figs. 7-8, respectively.

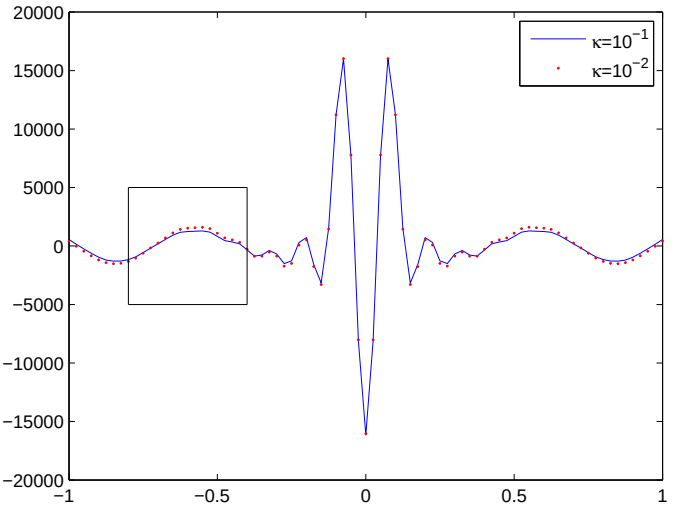

(a)

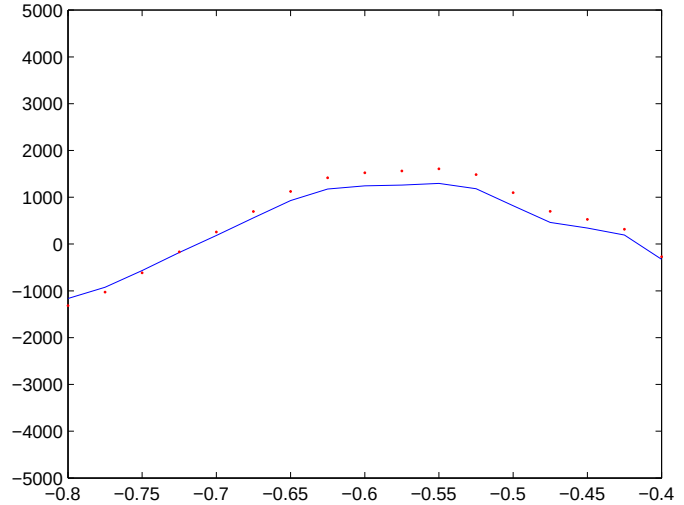

(b)

Figure 3: (a) $1D$ plot of $Im(E_2^1(x,x,0))$; (b) $1D$ plot of $Im(E_2^1(x,x,0))$ in rectangular region for $\kappa = 10^{-1}, 10^{-2}$

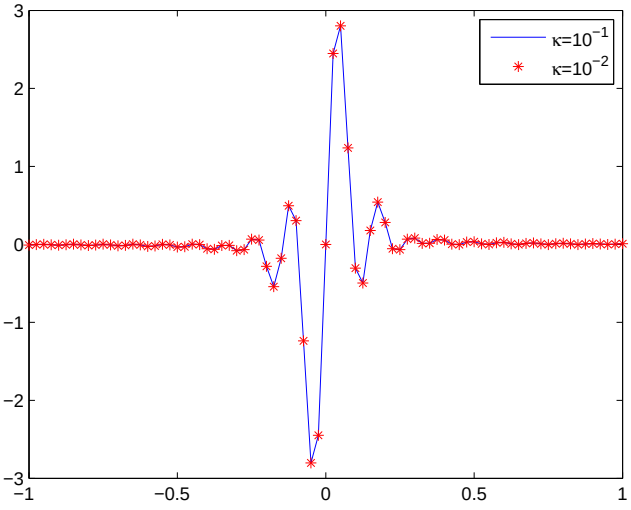

(a)

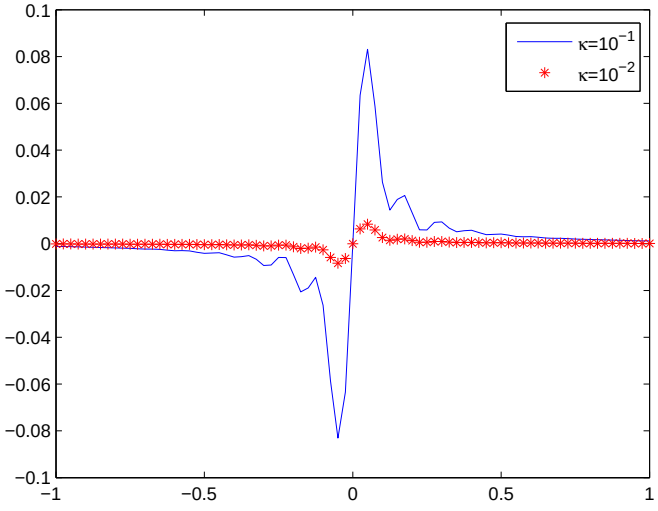

(b)

Figure 4: $\omega = 2c$, $\kappa = 10^{-1}, 10^{-2}$ (a) $2D$ plot of $Im(H_1^1(x,x,0))$; (b) $2D$ plot of $Re(H_1^1(x,x,0))$

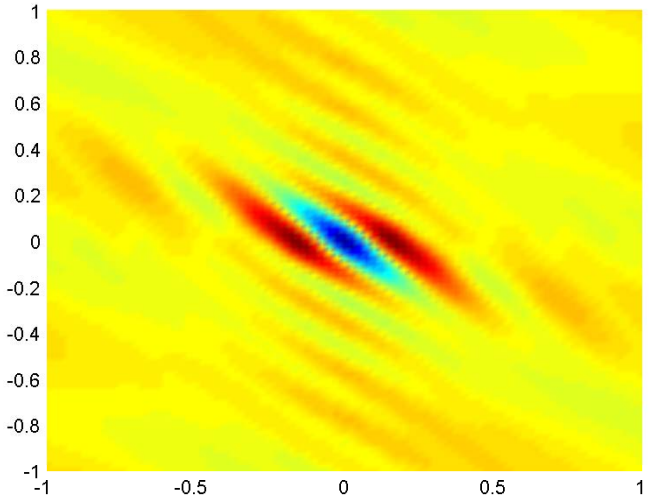

(a)

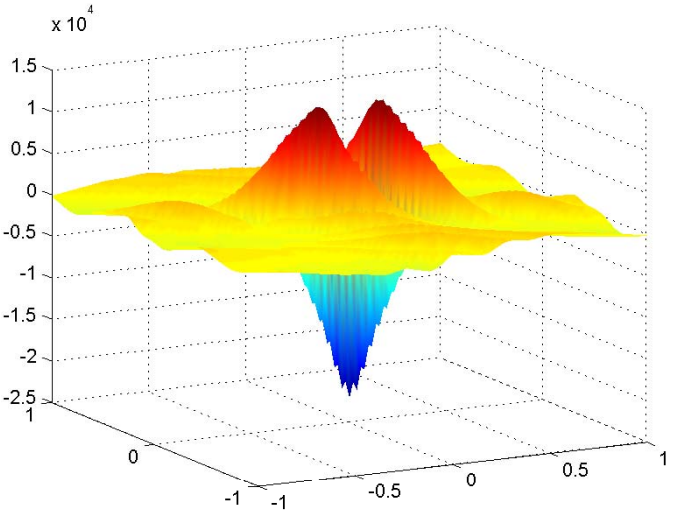

(b)

Figure 5: $\omega = 2c$, $\kappa = 10^{-1}$ (a) $2D$ plot of $Im(E_1^1(x_1,x_2,0))$; (b) $3D$ plot of $Im(E_1^1(x_1,x_2,0))$

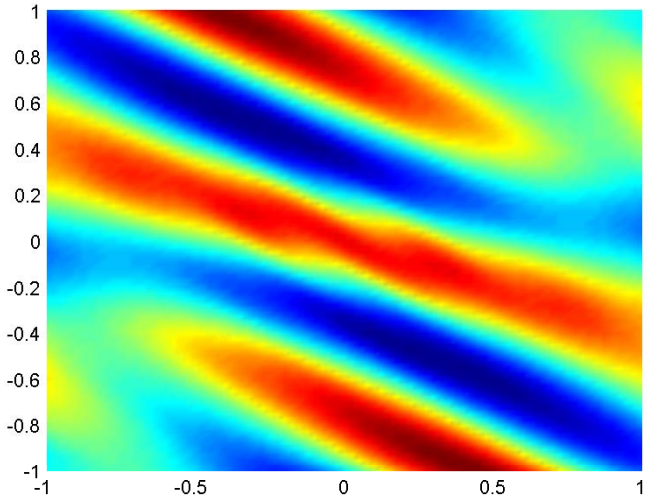

(a)

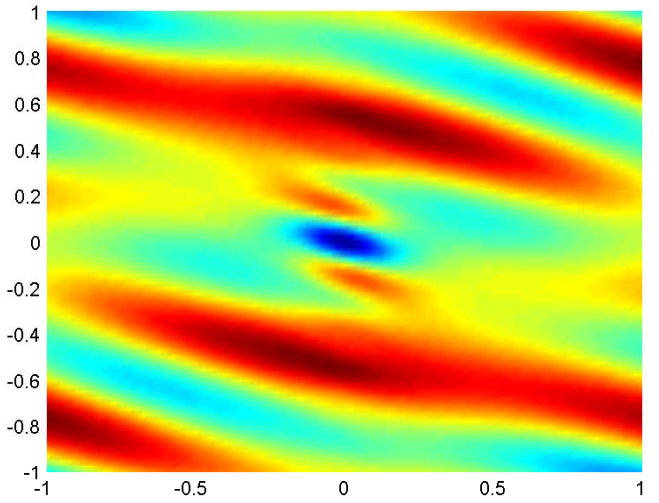

(b)

Figure 6: $\omega = 2c$, $\kappa = 10^{-1}$ (a) $2D$ plot of $Re(E_1^1(x_1,x_2,0))$; (b) $2D$ plot of $Re(E_2^1(x_1,x_2,0))$

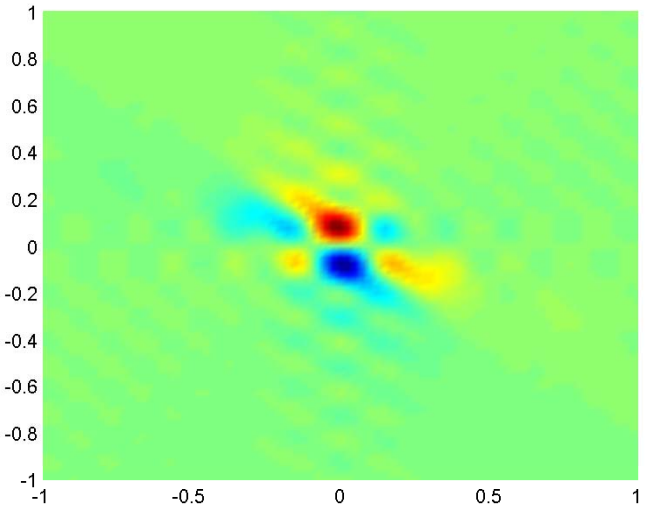

(a)

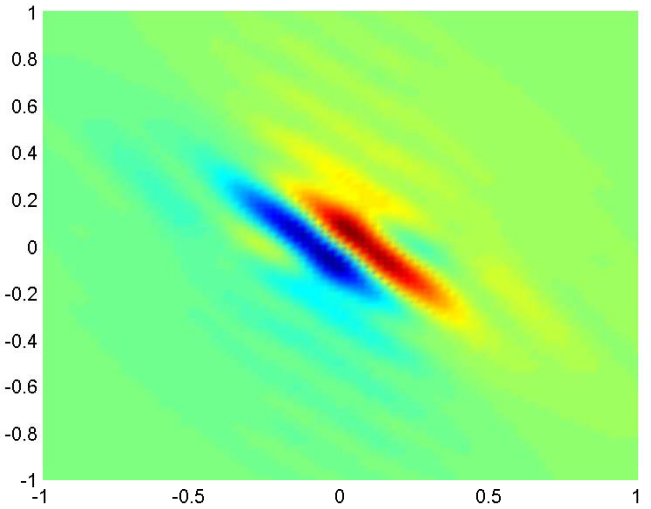

(b)

Figure 7: $\omega = 2c$, $\kappa = 10^{-1}$ (a) $2D$ plot of $Im(H_1^1(x_1,x_2,0))$; (b) $2D$ plot of $Re(H_1^1(x_1,x_2,0))$

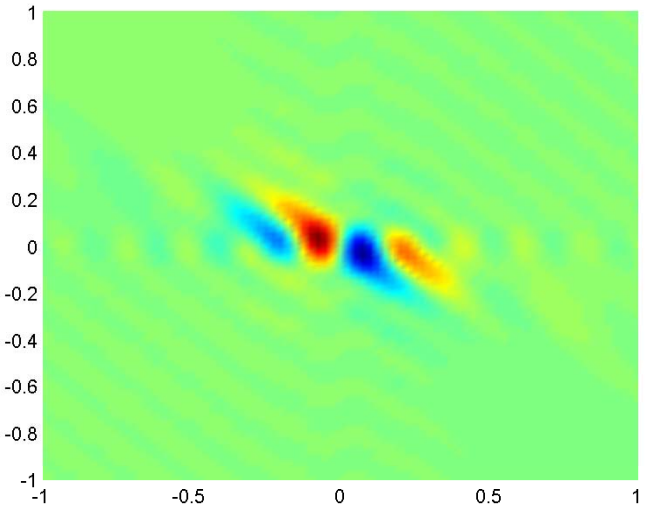

(a)

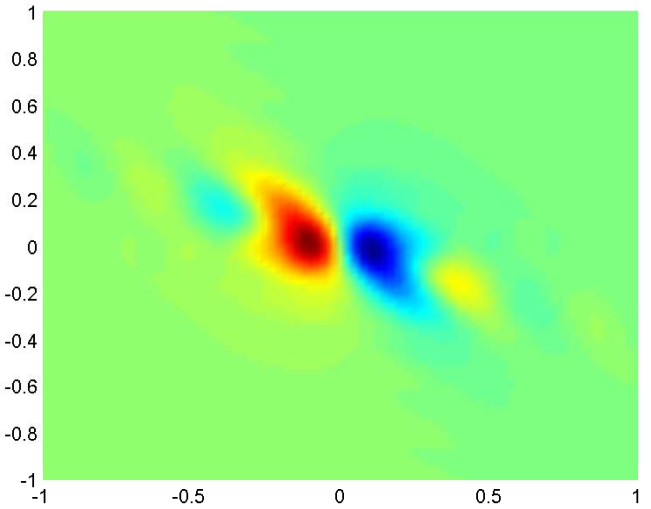

(b)

Figure 8: $\omega = 2c$, $\kappa = 10^{-1}$ (a) $2D$ plot of $Im(H_2^1(x_1,x_2,0))$; (b) $2D$ plot of $Re(H_2^1(x_1,x_2,0))$

In Fig. 3(a), the $1D$ plots of $Im(E_2^1(x,x,0))$ for $x_1 = x_2 = x, x_3 = 0$, $\omega = 2c$ for $\kappa = 10^{-1}$ and $\kappa = 10^{-2}$ is given. Fig. 3(b) presents the zoomed part of the graph of Fig. 3(a) in the indicated rectangle. Figs. 4(a), (b) present the $1D$ graphs of $Im(H_1^1(x_1,x_2,0))$ and $Re(H_1^1(x_1,x_2,0))$, respectively for $\kappa = 10^{-1}, 10^{-2}$. These graphs show the influence of κ on the components of the electric and magnetic Green's functions.

The behaviour of real and imaginary parts of the computed components of the electric and magnetic Green's functions is presented in Fig. 3, Figs. 5-6. The result of the simulation $Im(E_1^1(x_1,x_2,0))$ for $\omega = 2c$, $\kappa = 10^{-1}$ is presented in Fig. 5. The $3D$ plot of $Im(E_1^1(x_1,x_2,0))$ is shown in Fig. 5(b). Here the horizontal axes are x_1 and x_2, respectively. The vertical axis is the magnitude of $Im(E_1^1(x_1,x_2,0))$. Fig. 5(a) is a screen shot of $2D$ level plot of the same surface $Im(E_1^1(x_1,x_2,0))$, i.e. a view of the surface $z = Im(E_1^1(x_1,x_2,0))$ presented in Fig. 5(b) from the top of z-axis. Figs. 6(a), (b) illustrate the $2D$ level plots of $Re(E_1^1(x_1,x_2,0))$ and $Re(E_2^1(x_1,x_2,0))$, respectively.

The result of simulation $Im(H_1^1(x_1,x_2,0))$ and $Re(H_1^1(x_1,x_2,0))$ are presented in Fig. 7. Figs. 7(a), (b) are the $2D$ plots of $Im(H_1^1(x_1,x_2,0))$ and $Re(H_1^1(x_1,x_2,0))$ respectively. The illustration of $Im(H_2^1(x_1,x_2,0))$ and $Re(H_2^1(x_1,x_2,0))$ is given in Fig.8.

4 Conclusion

The method for the approximate computation of the electric and magnetic Green's functions for the time-harmonic Maxwell's equations in general gyro-electric materials has been developed in the paper. The method is based on the Fourier transform meta-approach. The Fourier transform with respect to the $3D$ space variable has been applied to partial differential equations for electric and magnetic Green's functions. The images of the Fourier transform of Green's functions were found from the obtained equations by the matrix transformations in MATLAB. The inverse Fourier transform of these images has been done numerically in the regularized (approximate) form in MATLAB. The parameters of this regularization have been chosen using the explicit formulae of the Green's function and its Fourier image for the Helmholtz equation. Two types of the computational experiments were presented in the paper. The first one demonstrates the high level of computational accuracy for the Fourier images and the inverse Fourier transform. The second one has been done for computing the electric and magnetic Green's functions in a general gyro-electric material. These computational experiments confirm the robustness of the method.

References

Barkleshli, S. (1993): Electromagnetic dyadic Green's function for multilayered symmetric gyro-electric media. *Radio Science*, vol. 28, no. 1, pp. 23–36.

Chen, J.; Ke, J. L. H. (2009): Construction of Green's function using field integral approach for Laplace problems with circular boundaries. *CMC: Com puters, Materials and Continua*, vol. 9, pp. 93–109.

Chew, W. C. (1990): *Waves and fields in inhomogeneous media*. New York: Van Nostrand Reinhold.

Ehrenpreis, L. (1960): Solution of some problems of division. *IV. Invertible and elliptic operators. Amer. J. Math.*, vol. 82, pp. 522–588.

Eroglu, A. (2010): *Wave Propagation and Radiation in Gyrotropic and Anisotropic Media*. Springer.

Eroglu, A.; Lee, J. K. (2003): Dyadic Green's function for a Gyro-electric Medium. *IEEE International*, vol. 2, pp. 1100–1103.

Eroglu, A.; Lee, J. K. (2006): Dyadic Green's function for an Electrically Gyrotropic medium. *PIER*, vol. 58, pp. 223–241.

Eroglu, A.; Lee, J. K. (2006): Wave propagation and dispersion characteristics for a nonreciprocal electrically gyrotropic medium. *PIER*, vol. 62, pp. 237–260.

Faraday, M. (1933): Faraday's Diary. *George Bell and Sons Ltd.*, vol. 4.

Freiser, M. J. (1968): A Survey of Magnetooptic Effects. *IEEE Transactions on Magnetics*, vol. 4, pp. 152–161.

Gu, M. H.; Young, D. L. F. C. M. (2009): The method of fundamental solutions for one-dimensional wave eqautions. *CMC: Com puters, Materials and Continua*, vol. 11, pp. 185–208.

Hormander, L. (1963): *Linear Partial Differential Operators*. Springer, Berlin.

Kong, J. A. (1984): *Electromagnetic Wave Theory*. John Wiley and Sons.

Lindell, I. V.; Sihvola, A. H. T. S. A. V. A. J. (1994): *Electromagnetic waves in chiral and biisotropic media*. New York: Artech House.

Malgrange, B. (1956): Existence et approximation des solutions des équations aux dérivées partielles et des équations de convolution. *Annales de l'institut Fourier*, vol. 6, pp. 271–355.

Olyslager, F. (1997): Time harmonic two- and three- dimensional closed form Green's dyadic for gyrotropic, bianisotropic, and anisotropic media. *Electromagnetics, Taylor and Fracis*, vol. 17, no. 4, pp. 369–386.

Ortner, N.; Wagner, P. (2004): Fundamental matrices of homogeneous hyperbolic systems. Applications to crystal optics, elastodynamics, and piezoelectromagnetism. *ZAMM Z. Angew. Math. Mech.*, vol. 84, no. 5, pp. 314–346.

Pershan, P. S. (1967): MagnetoOptical Effects. *Journal of Applied Physics*, vol. 38, pp. 1482.

Prati, E. (2003): Propagation in gyroelectromagnetic guiding system. *J. of Electromagn Waves and Appl.*, vol. 17, pp. 1177–1196.

Rashed, Y. F. (2004): Green's first identity method for boundary-only solution of self-weight in BEM formulation for thick slabs. *CMC: Com puters, Materials and Continua*, vol. 1, pp. 319–326.

Tai, C. T. (1994): *Dyadic Green's functions in electromagnetic theory*. New Jersey: IEEE Press.

Tewary, V.; Bartolo, L. P. A. (2002): Green's Functions Experts Meeting 274 and the GREEN Digital Library. *NIST Workshop Report.*

Tewary, V. K. (1995): Computationally efficient representation for elastodynamic and elastostatic Green's functions for anisotropic solids. *Physical Review B*, vol. 51, pp. 15695–15702.

Tewary, V. K. (2004): Elastostatic Green's function for advanced materials subject to surface loading. *Journal of Engineering Mathematics*, vol. 49, pp. 289–304.

Vladimirov, V. (1971): *Equations of Mathematical Physics*. Marcel Dekker, New York.

Vladimirov, V. (1979): *Generalized Functions in Mathematical Physics*. Mir, Moscow.

Wagner, P. (2011): The singular terms in the fundamental matrix of crystal optics. *Proc. R. Soc. A*, vol. 467, pp. 2663–2689.

Yakhno, V. G.; Ozdek, D. (2012): Computation of the time-dependent Green's function for the longitudinal vibration of multi-step rod. *CMES: Computer Modeling in Engineering and Sciences*, vol. 85, no. 2, pp. 157–176.

Yakhno, V. G.; Ozdek, D. (2013): The time-dependent Green's function of the transverse vibration of a composite multi stepped membrane. *CMC: Computers, Materials and Continua*, vol. 33, no. 2, pp. 155–173.

Yakhno, V. G.; Cerdik Yaslan, H. (2011): Computation of the time-dependent Green's function of three dimensional elastodynamics in 3D quasicrystals. *CMES: Computer Modeling in Engineering and Sciences*, vol. 81, no. 4, pp. 295–310.

Yakhno, V. G. (2008): Computing and simulation of time-dependent electromagnetic fields in homogeneous anisotropic materials. *International Journal of Engineering Science*, vol. 46, pp. 411–426.

Yakhno, V. G. (2011): Computation of Dyadic Green's Functions for Electrodynamics in Quasi-Static Approximation with Tensor Conductivity. *CMC: Computers, Materials and Continua*, vol. 21, no. 1, pp. 1–15.

Yang, B.; Tewary, V. K. (2008): Green's function for multilayered with interfacial membrane and flexural rigidities. *CMC: Computers, Materials and Continua*, vol. 8, pp. 23–31.

Young, D. L.; Chen, C. S. W. T. K. (2005): Solution of Maxwell's equations using the MQ method. *CMC: Computers, Materials and Continua*, vol. 2, pp. 267–276.

Appendix A: MATLAB code of computation of matrix $T(\nu)$ and $D(\nu)$

```
INPUT:Eps
[EigVecEps, EigValEps] = eig(Eps);
P = EigVecEps;
PT = P.';
M = EigValEps;
Mh = sqrt(M);
SqrEps = P*Mh*PT;
InvSrtEps = inv(SqrEps);
OUTPUT:SqrEps, InvSrtEps

INPUT:InvSrtEps, S0, SS
S0=zeros(3,3);
SS=[(v2*ndelta)^2+(v3*ndelta)^2 -(v1*ndelta)*(v2*ndelta)
-(v1*ndelta)*(v3*ndelta); -(v1*ndelta)*(v2*ndelta)
(v1*ndelta)^2+(v3*ndelta)^2 -(v2*ndelta)*(v3*ndelta);
-(v1*ndelta)*(v3*ndelta) -(v2*ndelta)*(v3*ndelta)
(v1*ndelta)^2+(v2*ndelta)^2];
S=[SS S0;S0 SS];
A=InvSrtEps*S*InvSrtEps;
[EigVecA,EigValA]=eig(A);
De=EigValA;
T=EigVecA;
[m,n]=size(T);
T1=zeros(m,n);
```

```
R=zeros(n,n);
for j=1:n
    v=T(:,j);
    for i=1:j-1
        R(i,j)=T1(:,i)'*T(:,j);
        v=v-R(i,j)*T1(:,i);
    end
    R(j,j)=norm(v);
    T1(:,j)=v/R(j,j);
end
T=InvSrtEps*Q1;
D=diag(De);
OUTPUT:T, D
```

Appendix B: MATLAB code of computation of matrix Q and $M(v)$

```
INPUT:Eps
Inveps=inv(Eps);
OUTPUT:Inveps

INPUT: InvEps, SC  SC=[0 -v3 v2; v3 0 -v1; -v2 v1 0];
S=SC*Inveps*SC;
Sr=real(S);
Si=imag(S);
SS=[Sr -Si; Si Sr];
[EigVecSS,EigValSS]=eig(SS);
De=EigValSS;
Q=EigVecSS;
[m,n]=size(Q);
Q1=zeros(m,n);
R=zeros(n,n);

for j=1:n
    v=Q(:,j);
    for i=1:j-1
        R(i,j)=Q1(:,i)'*Q(:,j);
        v=v-R(i,j)*Q1(:,i);
    end
    R(j,j)=norm(v);
```

```
    Q1(:,j)=v/R(j,j);
end
Q=Q1;

M=diag(De);
OUTPUT:Q, M
```